

# Nonlinear susceptibility of a quantum spin glass under uniform transverse and random longitudinal magnetic fields

S. G. Magalhaes<sup>1</sup>, C. V. Morais<sup>2</sup>, F. M. Zimmer<sup>3</sup>, M. J. Lazo<sup>4</sup>, F. D. Nobre<sup>5</sup>

<sup>1</sup>*Instituto de Física, Universidade Federal do Rio Grande do Sul, 91501-970 Porto Alegre, RS, Brazil\**

<sup>3</sup>*Instituto de Física e Matemática, Universidade Federal de Pelotas, 96010-900 Pelotas, RS, Brazil*

<sup>2</sup>*Departamento de Física, Universidade Federal de Santa Maria, 97105-900 Santa Maria, RS, Brazil*

<sup>4</sup>*Programa de Pós-Graduação em Física - Instituto de Matemática, Estatística e Física, Universidade Federal do Rio Grande, 96.201-900, Rio Grande, RS, Brazil and*

<sup>5</sup>*Centro Brasileiro de Pesquisas Físicas and National Institute of Science and Technology for Complex Systems, Rua Xavier Sigaud 150, 22290-180, Rio de Janeiro, RJ, Brazil*

(Dated: April 3, 2018)

The interplay between quantum fluctuations and disorder is investigated in a quantum spin-glass model, in the presence of a uniform transverse field  $\Gamma$ , as well as of a longitudinal random field  $h_i$ , which follows a Gaussian distribution characterized by a width proportional to  $\Delta$ . The interactions are infinite-ranged, and the model is studied through the replica formalism, within a one-step replica-symmetry-breaking procedure; in addition, the dependence of the Almeida-Thouless eigenvalue  $\lambda_{AT}$  (replicon) on the applied fields is analyzed. This study is motivated by experimental investigations on the  $\text{LiHo}_x\text{Y}_{1-x}\text{F}_4$  compound, where the application of a transverse magnetic field yields rather intriguing effects, particularly related to the behavior of the nonlinear magnetic susceptibility  $\chi_3$ , which have led to a considerable experimental and theoretical debate. We have analyzed two physically distinct situations, namely,  $\Delta$  and  $\Gamma$  considered as independent, as well as these two quantities related, as proposed recently by some authors. In both cases, a spin-glass phase transition is found at a temperature  $T_f$ , with such phase being characterized by a nontrivial ergodicity breaking; moreover,  $T_f$  decreases by increasing  $\Gamma$  towards a quantum critical point at zero temperature. The situation where  $\Delta$  and  $\Gamma$  are related [ $\Delta \equiv \Delta(\Gamma)$ ] appears to reproduce better the experimental observations on the  $\text{LiHo}_x\text{Y}_{1-x}\text{F}_4$  compound, with the theoretical results coinciding qualitatively with measurements of the nonlinear susceptibility  $\chi_3$ . In this later case, by increasing  $\Gamma$  gradually,  $\chi_3$  becomes progressively rounded, presenting a maximum at a temperature  $T^*$  ( $T^* > T_f$ ), with both the amplitude of the maximum and the value of  $T^*$  decreasing gradually. Moreover, we also show that the random field is the main responsible for the smearing of the nonlinear susceptibility, acting significantly inside the paramagnetic phase, leading to two regimes delimited by the temperature  $T^*$ , one for  $T_f < T < T^*$ , and another one for  $T > T^*$ . It is argued that the conventional paramagnetic state corresponds to  $T > T^*$ , whereas the temperature region  $T_f < T < T^*$  may be characterized by a rather unusual dynamics, possibly including Griffiths singularities.

Keywords: Spin Glasses, Critical Properties, Non-Linear Susceptibility, Replica-Symmetry Breaking.

PACS numbers: 75.10.Nr, 75.50.Lk, 05.70.Jk, 64.60.F-

## I. INTRODUCTION

Nature is quantum in its essence, although classical theories may be employed under certain conditions. In statistical mechanics, the temperature range becomes crucial for the use of classical or quantum approaches. Typical examples appear in magnetism, where the use of classical models is justified when the temperature ranges are high enough, when compared to some reference temperature. In many magnetic systems the quantum effects become relevant, and should be taken into account, like those within the realm of quantum magnetism<sup>1</sup>.

In what concerns spin glasses (SGs), models based on Ising variables have been able to describe fairly well, at least qualitatively, a wide variety of experimental behavior, even for sufficiently low temperatures<sup>2–5</sup>. Some of these results have been obtained at mean-field level, based on the infinite-range-interaction Sherrington-Kirkpatrick (SK) model<sup>6</sup>, either by means of the replica-

symmetric (RS), or replica-symmetry-breaking (RSB), solutions<sup>7</sup>. Although this may seem paradoxical, due to the fact that Ising SG Hamiltonians are not formulated in terms of quantum operators, it is understood since their binary variables capture an essential ingredient of many physical systems, for which strong anisotropy fields are present, leading to two significant states associated with the spin operators. However, in some compounds, the quantum fluctuations controlled by a given parameter (e.g., magnetic field, and/or doping) depress the transition temperature  $T_f$ , changing radically the physical properties of the system<sup>8</sup>. In some cases, a field transverse to such spin operators appears to be relevant, and so, the simpler Ising SG Hamiltonian should be replaced by a quantum type of Hamiltonian.

The Ising dipolar-coupled ferromagnet  $\text{LiHoF}_4$  is a well known system in which quantum fluctuations become important by applying a transverse magnetic field  $H_t$ , which induces quantum tunnelling through the bar-

rier separating the two degenerate ground states of  $\text{Ho}^{3+}$  ions<sup>9</sup>. Moreover, disorder can be introduced, by replacing the magnetic  $\text{Ho}^{3+}$  ions by nonmagnetic  $\text{Y}^{3+}$  ones. Therefore, the resulting  $\text{LiHo}_x\text{Y}_{1-x}\text{F}_4$  compound is considered as an ideal ground for investigating the interplay between quantum fluctuations and disorder in Ising spins systems<sup>10–12</sup>.

In these physical systems, coefficients of the expansion of the magnetization  $m$ , in powers of a small external longitudinal field  $H_l$ , are quantities of great interest<sup>2,3,13</sup>,

$$m = \chi_1 H_l - \chi_3 H_l^3 - \chi_5 H_l^5 - \dots, \quad (1)$$

corresponding to the linear susceptibility,

$$\chi_1 = \left. \frac{\partial m}{\partial H_l} \right|_{H_l \rightarrow 0}, \quad (2)$$

and nonlinear susceptibilities,

$$\chi_3 = -\frac{1}{3!} \left. \frac{\partial^3 m}{\partial H_l^3} \right|_{H_l \rightarrow 0}; \quad \chi_5 = -\frac{1}{5!} \left. \frac{\partial^5 m}{\partial H_l^5} \right|_{H_l \rightarrow 0}. \quad (3)$$

Since measurements of  $\chi_5$  (and higher-order susceptibilities) may become a hard task, very frequently in the literature one refers to  $\chi_3$  as the nonlinear susceptibility. Moreover,  $\chi_3$  is directly related to the SG susceptibility<sup>2,3</sup>,

$$\chi_3 = \beta^2 \left( \chi_{\text{SG}} - \frac{2}{3} \right), \quad (4)$$

with the latter representing an important theoretical tool, being defined as

$$\chi_{\text{SG}} = \frac{\beta}{N} \sum_{i,j} [(\langle S_i S_j \rangle - \langle S_i \rangle \langle S_j \rangle)^2]_{\text{av}}, \quad (5)$$

where  $\langle \dots \rangle$  and  $[\dots]_{\text{av}}$  denote, respectively, thermal averages and an average over the disorder.

In fact, the interplay between quantum fluctuations and disorder stands for the physical origin of the intriguing behavior found in the magnetic susceptibility  $\chi_3$  of  $\text{LiHo}_x\text{Y}_{1-x}\text{F}_4$ , which has been the object of a considerable experimental and theoretical debate. In the absence of  $H_t$ , the  $\text{LiHo}_{0.167}\text{Y}_{0.833}\text{F}_4$  compound displays a sharp peak in  $\chi_3$  at the temperature  $T_f$ , which resembles a conventional second-order SG phase transition<sup>14</sup>. Surprisingly, the sharp peak of  $\chi_3$  becomes increasingly rounded when the transverse field  $H_t$  is applied and enhanced, so that the resulting smooth curve presents a maximum located at a temperature  $T^*$ , with  $T^* > T_f$ . Such behavior was initially interpreted as a changing in the nature of the transition, from second order at  $T_f$  to first order at  $T^*$ <sup>14,15</sup>. More recently, Jönsson and collaborators<sup>16</sup> investigated the behavior of  $\chi_3$  for dopings  $x = 0.165$  and  $0.0045$ , obtaining the same roundings of the peak in both cases; these authors understood this behavior as an evidence of absence of a SG phase transition

of any nature. In contrast, Ancona-Torres and collaborators<sup>17</sup> performed measurements for doping  $x = 0.167$ , not only of  $\chi_3$ , but also of  $\chi_5$ , as well as of the ac susceptibility, reasserting  $T^*$  as the SG critical temperature.

On the theoretical side, the debate on this particular issue has also been intense (see, for instance, Refs.<sup>18,19</sup>). The suggestion that an effective longitudinal random field (RF)  $h_i$  can be induced from the interplay of a transverse applied field  $H_t$ , with the off-diagonal terms of the dipolar interactions in  $\text{LiHo}_x\text{Y}_{1-x}\text{F}_4$ , represents a very interesting hint to clarify these controversies concerning the meaning of  $T^{*20-24}$ . According to the droplet picture for SGs, the rounded behavior of  $\chi_3$  in the presence of the field-induced RF  $h_i$  is interpreted as a suppression of the SG transition<sup>20,21</sup>, similar to what a uniform field does in that picture<sup>25,26</sup>. On the other hand, Tabei and collaborators<sup>22</sup> working within Parisi's mean-field theory<sup>7</sup>, using an effective Hamiltonian defined in terms of the field-induced RF  $h_i$  and a transverse field  $\Gamma$  [where  $\Gamma = \Gamma(H_t)$  represents some monotonically increasing function of  $H_t$ ], reproduced quite well the experimental behavior of  $\chi_3$ , with an increasingly rounded peak at  $T^*$  when  $H_t$  is enhanced.

It should be remarked that the results described above are based on a particular approach of the quantum SK model proposed by Kim and collaborators<sup>27</sup>. In this approach, the SK model is analyzed in the presence of a transverse field  $\Gamma$ , within the static approximation. Mostly important, a region inside the SG phase was found where the RS approximation is stable. Actually, the RSB solution exists only for sufficiently low values of  $\Gamma$ , at temperatures lower than the SG transition temperature. The main consequence of this scenario is that the sharp peak of  $\chi_3$ , which signals the SG phase transition temperature, does not coincide with the onset of RSB. Nevertheless, this result is also highly controversial, since other works indicate precisely the opposite, i.e., the RS approximation is unstable throughout the whole SG phase (see, for instance, Refs.<sup>28,29</sup>) except, possibly, at the zero-temperature Quantum Critical Point (QCP)<sup>30</sup>. Consequently, when  $\Gamma$  enhances, the RSB transition temperature  $T_f$  decreases, so that, for finite temperatures, the critical behavior appears in  $\chi_3$  as

$$\chi_3 \propto [(\Gamma - \Gamma_f(T))/\Gamma_f(T)]^{-\delta'}, \quad (6)$$

where  $\Gamma_f(T)$  denotes the critical value of  $\Gamma$  for a given temperature, from which its corresponding value at the zero-temperature QCP is obtained as  $\lim_{T \rightarrow 0} \Gamma_f(T) = \Gamma_c^0$ .

In the classical case, it is well known that  $\chi_{\text{SG}}$  is inversely proportional to the Almeida-Thouless eigenvalue  $\lambda_{\text{AT}}$ , the so-called replicon<sup>2,31</sup>. Therefore, the diverging behavior of  $\chi_3$  at the SG transition,

$$\chi_3 \propto [(T - T_f)/T_f]^{-\gamma}, \quad (7)$$

is a direct consequence of  $\lambda_{\text{AT}} = 0$  at  $T_f$ , occurring together with the onset of RSB. Similarly, in the quan-

tum case, one expects that the divergence of  $\chi_3$  at  $\Gamma_f(T)$  should coincide with the onset of RSB.

Indeed, the presence of a RF can produce deep changes in the scenario described previously. For instance, in the classical SK model<sup>6</sup>, the RF induces the RS order parameter  $q$ , which becomes finite at any temperature<sup>32,33</sup>. As a consequence,  $q$  versus temperature presents a smooth behavior, being no more appropriate for identifying a SG transition in the SK model. Nevertheless, such a transition may still be related with the onset of RSB, signaled by  $\lambda_{AT} = 0$ <sup>34</sup>. In spite of this, the derivative of  $q$  with respect to the temperature increases as one approaches  $T_f$  from above; such an increase is the ultimate responsible for the rounded maximum in  $\chi_3$  at the temperature  $T^*$ , which does not coincide with the SG transition temperature  $T_f$  ( $T^* > T_f$ ). In fact, the maximum value of  $\chi_3$  at  $T^*$  reflects the effects of the RF inside the paramagnetic phase, instead of the non-trivial ergodicity breaking of the SG phase transition<sup>35</sup>. Therefore, one can raise the question of whether such scenario for  $\chi_3$ , found in the classical SK model, is robust in the corresponding quantum model, when the transverse field is considered, i.e.,  $\Gamma \neq 0$ , and no longer independent from the RF, as proposed by Tabei and collaborators<sup>22</sup>.

The purpose of the present work is to study the susceptibility  $\chi_3$ , using the so-called fermionic Ising SG model in the presence of a longitudinal RF  $h_i$  and a transverse field  $\Gamma$ . In this model, the spin operators are written in terms of fermionic occupation and destruction operators<sup>36,37</sup>, whereas the spin-spin couplings  $\{J_{ij}\}$  and random fields  $\{h_i\}$  follow Gaussian distributions. The grand-canonical potential is obtained in the functional integral formalism, and the disorder is treated using the replica method; moreover, the SG order parameters are obtained in the static approximation<sup>38,41</sup> and investigated within the one-step RSB scheme<sup>7</sup>. It should be remarked that the fermionic Ising SG model is defined on the Fock space, where there are four possible states per site: one state with no fermions, two states with a single fermion, and one state with two fermions, leading to two nonmagnetic states. In particular, one can consider two cases: the  $4S$  model that allows the four possible states per site and the  $2S$  model, which restricts the spin operators to act on a space where the nonmagnetic states are forbidden. In the present work we will consider the later model, by imposing a restriction to remove the contribution of these nonmagnetic states, i.e., taking into account only the sites occupied by one fermion in the partition-function trace<sup>39,40</sup>.

In order to deal appropriately with the experimental behavior of  $\chi_3$  in the  $\text{LiHo}_x\text{Y}_{1-x}\text{F}_4$  compound, we focus our calculations on the  $2S$  model by proposing a relationship between  $\Delta$  (the width of the distribution of random fields  $h_i$ ) and  $\Gamma$ , following the approach introduced by Tabei and collaborators<sup>22</sup>. The main characteristic observed experimentally in  $\chi_3$  concerns the peak for small  $H_t$  (classical limit) being replaced by a rounded maximum which becomes increasingly rounded for large  $H_t$

(quantum limit). Besides the progressive smearing of  $\chi_3$ , the amplitude of its maximum also decreases as  $H_t$  increases. Therefore, the effects of the RF triggered by  $H_t$ , as suggested by Tabei and collaborators<sup>22</sup>, should provoke simultaneously both effects, i.e., the smearing of the peak and the decrease of the maximum amplitude value of  $\chi_3$ . For the present fermionic Ising SG model, we have tested a relationship involving  $\Delta$  and  $\Gamma$ , particularly in the power-like form,  $\Delta/J \propto (\Gamma/J)^{B'}$ , where  $J$  represents the width of the Gaussian distribution for the couplings  $\{J_{ij}\}$ . Considering the interval for the exponent,  $1.8 < B' < 2.5$ , we have been able to obtain  $\chi_3$  as a function of temperature and  $\Gamma$  resembling qualitatively the experimental behavior for  $\chi_3$  described above. As already mentioned, the transverse field  $\Gamma$  used in the effective model to describe  $\text{LiHo}_x\text{Y}_{1-x}\text{F}_4$  is expected to be related to the experimental applied field  $H_t$ <sup>11,12</sup>; in fact, at least for low  $H_t$ ,  $\Gamma \propto H_t^2$  (see, e.g., Ref.<sup>42</sup>).

The paper is structured as follows: in Section II we define the model and find its grand-canonical potential within the one-step RSB scheme; in Section III we present a detailed discussion of the order parameters, the susceptibility  $\chi_3$ , and some phase diagrams. Finally, the last section is reserved to conclusions.

## II. MODEL

The model is defined by the Hamiltonian

$$H = - \sum_{(i,j)} J_{ij} \hat{S}_i^z \hat{S}_j^z - \sum_{i=1}^N h_i \hat{S}_i^z - 2\Gamma \sum_{i=1}^N \hat{S}_i^x, \quad (8)$$

where the summation  $\sum_{(i,j)}$  applies to all distinct pairs of spin operators, whereas the couplings  $\{J_{ij}\}$  and magnetic fields  $\{h_i\}$  are quenched random variables, following independent Gaussian distributions,

$$P(J_{ij}) = \left[ \frac{N}{32\pi J^2} \right]^{1/2} \exp \left[ -\frac{N}{32J^2} (J_{ij} - J_0/N)^2 \right], \quad (9)$$

and

$$P(h_i) = \left[ \frac{1}{32\pi \Delta^2} \right]^{1/2} \exp \left[ -\frac{1}{32\Delta^2} h_i^2 \right]. \quad (10)$$

In order to obtain susceptibilities [cf. Eqs. (2) and (3)], one introduces a longitudinal uniform field  $H_t$ , by adding an extra term  $-\sum_{i=1}^N H_t \hat{S}_i^z$  in the Hamiltonian above. Moreover, the spin operators in Eq. (8) are defined as

$$\hat{S}_i^z = \frac{1}{2}[\hat{n}_{i\uparrow} - \hat{n}_{i\downarrow}]; \quad \hat{S}_i^x = \frac{1}{2}[\hat{c}_{i\uparrow}^\dagger \hat{c}_{i\downarrow} + \hat{c}_{i\downarrow}^\dagger \hat{c}_{i\uparrow}], \quad (11)$$

where  $\hat{n}_{i\uparrow} = \hat{c}_{i\uparrow}^\dagger \hat{c}_{i\uparrow}$  and  $\hat{n}_{i\downarrow} = \hat{c}_{i\downarrow}^\dagger \hat{c}_{i\downarrow}$ , with  $\hat{c}_{i\uparrow}^\dagger$  denoting a creation operator for a fermion with spin up at site  $i$ ,  $\hat{c}_{i\downarrow}$  an annihilation operator for a fermion with spin down at site  $i$ , and so on. In this fermionic problem, the partition

function is expressed by using the Lagrangian path integral formalism in terms of anticommuting Grassmann fields ( $\phi$  and  $\phi^*$ )<sup>37</sup>. The restriction in the 2S-model is imposed by means of a Kronecker delta function, in such a way to take into account only those sites occupied by one fermion ( $n_{i\uparrow} + n_{i\downarrow} = 1$ ) in the partition-function<sup>39,40</sup>. Therefore, adopting an integral representation for this delta function, one can express the partition function for both 2S and 4S models in the following form,

$$Z\{y\} = e^{\frac{s-2}{2}N\beta\mu} \int D(\phi^*\phi) \prod_j \frac{1}{2\pi} \int_0^{2\pi} dx_j e^{-y_j} e^{A\{y\}}, \quad (12)$$

where

$$A\{y\} = \int_0^\beta d\tau \left\{ \sum_{j,\sigma} \phi_{j\sigma}^*(\tau) \left[ \frac{\partial}{\partial \tau} + \frac{y_j}{\beta} \right] \phi_{j\sigma}(\tau) - H(\phi_{j\sigma}^*(\tau), \phi_{j\sigma}(\tau)) \right\}. \quad (13)$$

In the equations above,  $\beta = 1/T$  ( $T$  being the temperature),  $y_j = ix_j$  for the 2S-model, or  $y_j = \beta\mu$  for the 4S-model,  $s = 2, 4$  denotes the number of states per site allowed in each model, respectively, and  $\mu$  is the chemical potential. Moreover,  $\phi_{j\sigma}$  and  $\phi_{j\sigma}^*$  represent Grassmann fields at site  $j$  and spin state  $\sigma$ , whereas  $H(\phi_{j\sigma}^*(\tau), \phi_{j\sigma}(\tau))$  stands for an effective Hamiltonian at a given value of the integration variable  $\tau$ .

Now, we use the replica method, so that standard procedures lead to the grand-canonical potential per particle<sup>25</sup>,

$$\beta\Omega = -\frac{1}{N} \langle \ln Z\{y\} \rangle_{J,h} = -\frac{1}{N} \lim_{n \rightarrow 0} \frac{\langle \langle Z\{y\}^n \rangle \rangle_{J,h} - 1}{n}, \quad (14)$$

where  $\langle \langle \dots \rangle \rangle_{J,h}$  denote averages over the quenched random variables. The replicated partition function  $\langle \langle Z\{y\}^n \rangle \rangle_{J,h}$  becomes

$$\begin{aligned} \langle \langle Z\{y\}^n \rangle \rangle_{J,h} &= e^{\frac{s-2}{2}N\beta\mu} \mathcal{N} \int_{-\infty}^{\infty} \prod_{(\alpha,\gamma)} dq_{\alpha\gamma} \int_{-\infty}^{\infty} \prod_{\alpha=1}^n dq_{\alpha\alpha} \\ &\times \int_{-\infty}^{\infty} \prod_{\alpha=1}^n dm_{\alpha} \exp [N\beta\Omega_n(q_{\alpha\gamma}, q_{\alpha\alpha}, m_{\alpha})] \end{aligned} \quad (15)$$

where  $\alpha$  ( $\alpha = 1, 2, \dots, n$ ) stands for a replica index,  $(\alpha, \gamma)$  denotes distinct pairs of replicas, and  $\mathcal{N} = (\beta J \sqrt{N/2\pi})^{n(n+1)/2}$ . Assuming the static approximation<sup>38,41</sup>, one obtains

$$\begin{aligned} \beta\Omega_n(q_{\alpha\gamma}, q_{\alpha\alpha}, m_{\alpha}) &= -\beta^2 J^2 \sum_{(\alpha,\gamma)} q_{\alpha\gamma}^2 \\ &- \frac{\beta^2 J^2}{2} \sum_{\alpha} q_{\alpha\alpha}^2 - \frac{\beta J_0}{2} \sum_{\alpha} m_{\alpha}^2 + \ln \Lambda\{y\}, \end{aligned} \quad (16)$$

and the Fourier representation may be used to express

$$\Lambda\{y\} = \prod_{\alpha} \frac{1}{2\pi} \int_0^{2\pi} dx_{\alpha} e^{-y_{\alpha}} \int D[\phi_{\alpha}^*, \phi_{\alpha}] \exp[H_{\text{eff}}]. \quad (17)$$

Above, one has an “effective Hamiltonian” in replica space,

$$\begin{aligned} H_{\text{eff}} &= \sum_{\alpha} A_{0\Gamma}^{\alpha} + 4 \left[ \frac{\beta^2 \Delta^2}{2} \sum_{\alpha,\gamma} S_{\alpha}^z S_{\gamma}^z + \frac{\beta J_0}{2} \sum_{\alpha} m_{\alpha} S_{\alpha}^z \right. \\ &\quad \left. + \beta^2 J^2 \left( \sum_{\alpha} q_{\alpha\alpha} S_{\alpha}^z S_{\alpha}^z + 2 \sum_{(\alpha,\gamma)} q_{\alpha\gamma} S_{\alpha}^z S_{\gamma}^z \right) \right], \end{aligned} \quad (18)$$

with

$$\begin{aligned} A_{0\Gamma}^{\alpha} &= \sum_{\omega} \varphi_{\alpha}^{\dagger}(\omega) (i\omega + y_{\alpha} + \beta\Gamma \underline{\sigma}^x) \varphi_{\alpha}(\omega), \\ S_{\alpha}^z &= \frac{1}{2} \sum_{\omega} \varphi_{\alpha}(\omega) \underline{\sigma}^z \varphi_{\alpha}(\omega), \end{aligned} \quad (19)$$

where the Matsubara’s frequencies are  $\omega = \pm\pi, \pm 3\pi, \dots$ ,  $\underline{\sigma}^x$  and  $\underline{\sigma}^z$  denote the Pauli matrices, and  $\varphi_{\alpha}^{\dagger}(\omega) = (\phi_{\uparrow\alpha}^*(\omega) \ \phi_{\downarrow\alpha}^*(\omega))$ .

Moreover, the functional integrals over  $q_{\alpha\gamma}$ ,  $q_{\alpha\alpha}$  and  $m_{\alpha}$  in Eq. (15) have been evaluated through the steepest-descent method, yielding

$$m_{\alpha} = \langle S_{\alpha} \rangle; \quad q_{\alpha\gamma} = \langle S_{\alpha}^z S_{\gamma}^z \rangle; \quad q_{\alpha\alpha} = \langle (S_{\alpha}^z)^2 \rangle, \quad (20)$$

with  $\langle \dots \rangle$  representing a thermal average over the effective Hamiltonian of Eq. (18).

Herein, the problem will be analyzed within one-step RSB Parisi’s scheme<sup>7</sup>, in which  $q_{\alpha\alpha} = p$ , and the replica matrix elements are parametrized as

$$q_{\alpha\gamma} = \begin{cases} q_1 & \text{if } I(\alpha/a) = I(\gamma/a) \\ q_0 & \text{if } I(\alpha/a) \neq I(\gamma/a) \end{cases} \quad (21)$$

where  $I(x)$  gives the smallest integer greater than, or equal to  $x$ .

The parametrization given by Eq. (21) allows to perform the sums over replica indexes and then, the quadratic terms in Eq. (18) can be linearized through the introduction of new auxiliary fields. From this point, the integrals over the Grassmann variables in Eq. (17) can be performed and the sum over Matsubara’s frequencies can be obtained, like in Ref.<sup>40</sup>. Therefore, the resulting grand-canonical potential is obtained from Eq. (14),

$$\begin{aligned} \beta\Omega &= \frac{(\beta J)^2}{2} [(x-1)q_1^2 - xq_0^2 + p^2] + \frac{\beta J_0}{2} m^2 - \ln 2 \\ &- \frac{(s-2)}{2} \beta\mu - \frac{1}{x} \int Dv \ln \left\{ \int Dv [K(z, v)]^x \right\}, \end{aligned} \quad (22)$$



where

$$\begin{aligned}
K(z, v) &= \frac{(s-2)}{2} \cosh(\beta\mu) + \int D\xi \cosh[\sqrt{\Xi(z, v, \xi)}], \\
\Xi(z, v, \xi) &= [\beta h(z, v, \xi)]^2 + (\beta\Gamma)^2, \\
h(z, v, \xi) &= \beta J [\sqrt{2q_0 + (\Delta/J)^2} z + \sqrt{2(q_1 - q_0)} v \\
&\quad + \sqrt{2(p - q_1)} \xi],
\end{aligned} \tag{23}$$

and  $Dx \equiv dx e^{-x^2/2}/\sqrt{2\pi}$  ( $x = z, v$  or  $\xi$ ).

The parameters  $q_0$ ,  $q_1$ ,  $x$ ,  $p$ , and  $m$  are obtained through extremization of the grand-canonical potential in Eq. (22), and results for 2S and 4S models are obtained by considering  $s = 2$  and  $s = 4$ , respectively. Moreover, the RS solution is recovered for  $q_0 = q_1 = q$ , and  $x = 0$ . In this way, the linear susceptibility of Eq. (2) becomes  $\chi_1 = \beta[p - q_1 + x(q_1 - q_0)]^7$ .

As usual, the RSB parameters, the magnetization  $m$ , and the quadrupolar parameter  $p$ , form a set of coupled equations, to be solved simultaneously. Particularly, the parameter  $p$  is quite dependent on  $\Gamma$ , and in fact, for the 2S model,  $p \rightarrow 1$  only as  $\Gamma \rightarrow 0$ ; it should be mentioned that  $p$  plays an important role in the nonlinear susceptibility  $\chi_3$ . This aspect represents a crucial difference of the present investigation with respect to previous one, by Kim and collaborators [cf. Ref.<sup>27</sup>], where the parameters  $q_1$ ,  $q_0$ , and  $x$  (or even  $q$  in the RS solution) do not depend on  $p$ . In the present work, for the above one-step RSB solution,  $\chi_3$  will be obtained by numerical derivatives; for the RS solution, an analytical form for  $\chi_3$  is presented in Appendix A. As mentioned before, in order to deal with the  $\text{LiHo}_x\text{Y}_{1-x}\text{F}_4$  compound, we will restrict ourselves to the 2S model, considering  $J_0 = 0$ .

### III. RESULTS

Hence, considering the 2S model, in this section we analyze the behavior of the nonlinear susceptibility  $\chi_3$ , either by varying the temperature (for fixed typical values of  $\Delta/J$  and  $\Gamma/J$ ), or by considering joint variations in some of these parameters. Since  $\chi_3$  is directly related with the order parameters that appear in the thermodynamic potential of Eq. (22), we first discuss the SG order parameters  $q_1$  and  $q_0$ , as well as the quadrupolar parameter  $p$ . Moreover, the onset of RSB is signalled by  $\delta = q_1 - q_0 > 0$ , which locates the freezing temperature  $T_f$ ; it should be mentioned that for  $\Gamma = 0$  and  $\Delta = 0$ , one has that  $T_f = \sqrt{2}J$ .

In Fig. 1 we exhibit the one-step RSB parameter  $\delta \equiv q_1 - q_0$  versus the dimensionless temperature  $T/J$ , for typical choices of  $\Gamma/J$  and  $\Delta/J$ . The corresponding parameters  $q_1$ ,  $q_0$ , and  $p$  are also presented versus  $T/J$  in the respective insets. From Fig. 1(a) one notices that the freezing temperature gets lowered for increasing values of the transverse field  $\Gamma$ , up to the zero-temperature QCP located at  $\Gamma_c^0 = 2\sqrt{2}J$  ( $\Delta = 0$ )<sup>40</sup>; a similar effect is

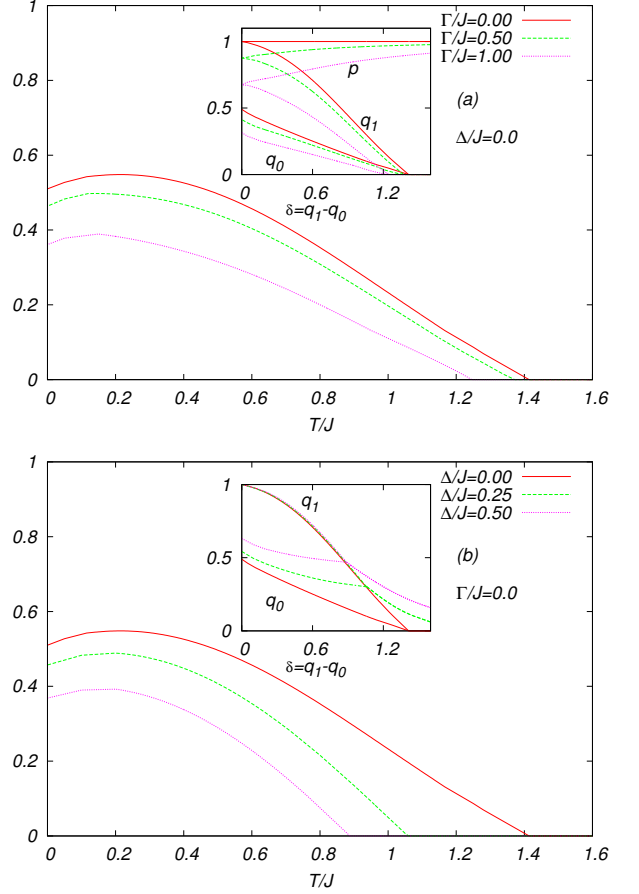


FIG. 1: The one-step RSB parameter  $\delta \equiv q_1 - q_0$  is presented versus the dimensionless temperature  $T/J$ , for  $\Delta = 0$  and typical values of  $\Gamma/J$  [panel (a)], as well as for  $\Gamma = 0$  and typical values  $\Delta/J$  [panel (b)]. The parameters  $q_1$ ,  $q_0$ , and  $p$  are also exhibited versus temperature in the respective insets; one notices that the quadrupolar parameter  $p$  becomes relevant only in the cases  $\Gamma > 0$ , for which it decreases by lowering the temperature. Due to the usual numerical difficulties, the low-temperature results [typically  $(T/J) < 0.05$ ] correspond to smooth extrapolations from higher-temperature data.

verified in Fig. 1(b) by increasing the width of the distribution of random fields  $\Delta$  ( $\Gamma = 0$ ). In the Hamiltonian of Eq. (8) one sees that the limit  $\Gamma = 0$  corresponds to a simple, diagonalizable, quantum Ising SG model, where only the spin components  $\hat{S}_i^z$  are present, leading to a trivial quadrupolar parameter  $p = 1$  (for all temperatures), as shown in the inset of Fig. 1(a). This particular case, for which the SG parameters are exhibited in Fig. 1(b), yields results qualitatively similar to those found in the previous study of the classical SK model in the presence of a Gaussian random field, carried in Ref.<sup>35</sup>. One notices that for  $(\Delta/J) > 0$  the RS order parameter  $q = q_0 = q_1$  is induced [cf. the inset of Fig. 1(b)], presenting a smooth behavior versus temperature; consequently, the freezing temperature  $T_f$  can only be found by means of the RSB scheme, with the SG transition coinciding with the onset of the parameter  $\delta$ . However, for  $\Gamma > 0$ , the spin

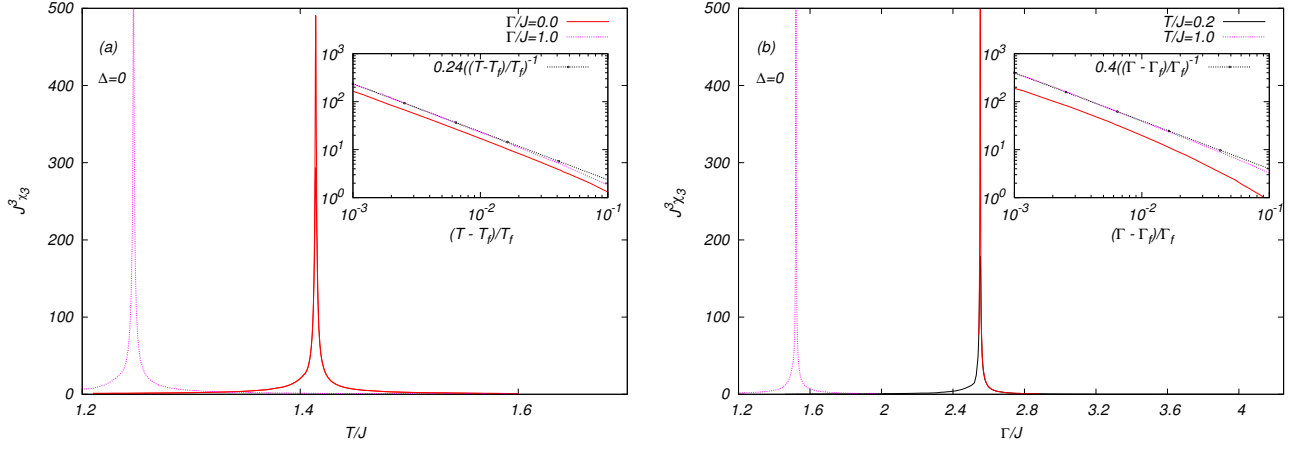


FIG. 2: Plots of the dimensionless nonlinear susceptibility [computed from Eq. (3)] are exhibited for  $\Delta = 0$ : (a)  $J^3\chi_3$  versus  $T/J$  for two different values of  $\Gamma/J$ ; (b)  $J^3\chi_3$  versus  $\Gamma/J$  for two different temperatures. In all cases one notices sharp divergences of  $\chi_3$ , signaling evident phase transitions. The corresponding critical exponents are estimated through log-log plots (shown in the respective insets), where in each case, the fitting proposal is represented by a dashed-dotted line (see text).

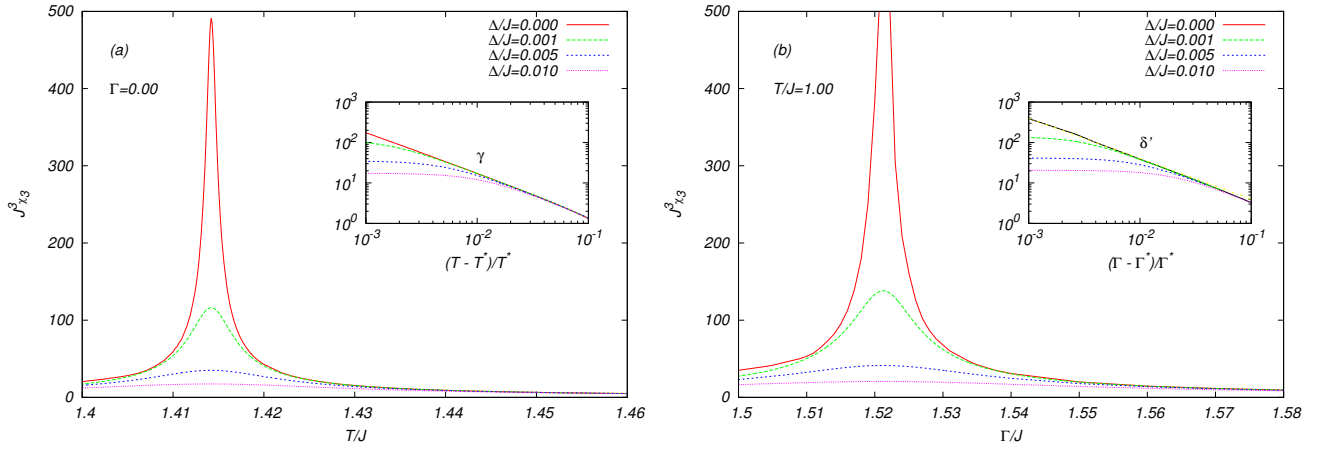


FIG. 3: The behavior of the dimensionless nonlinear susceptibility (in two typical cases exhibited in Fig. 2) is presented for increasing values of  $\Delta/J$ : (a)  $J^3\chi_3$  versus  $T/J$ , for  $(\Gamma/J) = 0.0$ ; (b)  $J^3\chi_3$  versus  $\Gamma/J$ , for  $(T/J) = 1.0$ . In each case one notices a rounded peak for  $(\Delta/J) > 0$ , with its maximum value located at a temperature  $T^*$  [panel (a)], or at a transverse field  $\Gamma^*$  [panel (b)], such that its height decreases for increasing values of  $\Delta/J$ . The log-log plots in the respective insets show that the divergences of Eq. (7), leading to the exponent  $\gamma$  [inset of (a)], or in Eq. (6), leading to the exponent  $\delta'$  [inset of (b)], are fulfilled only for  $(\Delta/J) = 0$ .

components  $\hat{S}_i^x$  become important, so that one expects a nontrivial behavior for the quadrupolar parameter  $p$ ; indeed,  $p$  should decrease for increasing values of  $\Gamma$  (at a fixed temperature), whereas for a fixed  $\Gamma$ , it decreases by lowering the temperature, as shown in the inset of Fig. 1(a).

In the present problem, clear phase transitions may be verified only for  $\Delta = 0$ , like those exhibited in Fig. 2. From the  $\chi_3$  plots of Fig. 2(a) one confirms two important features shown in Fig. 1(a), concerning the behavior of the order parameters  $q_0$ ,  $q_1$  and  $\delta$ : (i) The freezing temperature  $T_f$ , signaled by the divergence of  $\chi_3$  in Fig. 2(a), coincides with the onset of RSB indicated by the parameter  $\delta$  of Fig. 1(a); (ii) The temperature

$T_f$  is lowered by increasing values of  $\Gamma/J$ . The critical exponents associated with the divergences of  $\chi_3$  may be obtained by log-log plots, as shown in the insets of Fig. 2. In the inset of Fig. 2(a) we have verified that the behavior of Eq. (7) (represented by the dashed-dotted line) fits well the region  $0.001 < (T - T_f)/T_f < 0.1$ , with the same critical exponent,  $\gamma = 1$ , for both values  $\Gamma/J = 0.0$  (full line) and  $\Gamma/J = 1.0$  (dotted line), suggesting that the transverse field  $\Gamma$  should not change the universality class of the exponent  $\gamma$ . It is important to mention that this estimate coincides with the well-known value found for the SK model<sup>2</sup>. In Fig. 2(b) one sees divergences of  $\chi_3$  at given values of  $\Gamma$  [defined as  $\Gamma_f(T)$  in Eq. (6)], for two typical fixed temperatures;

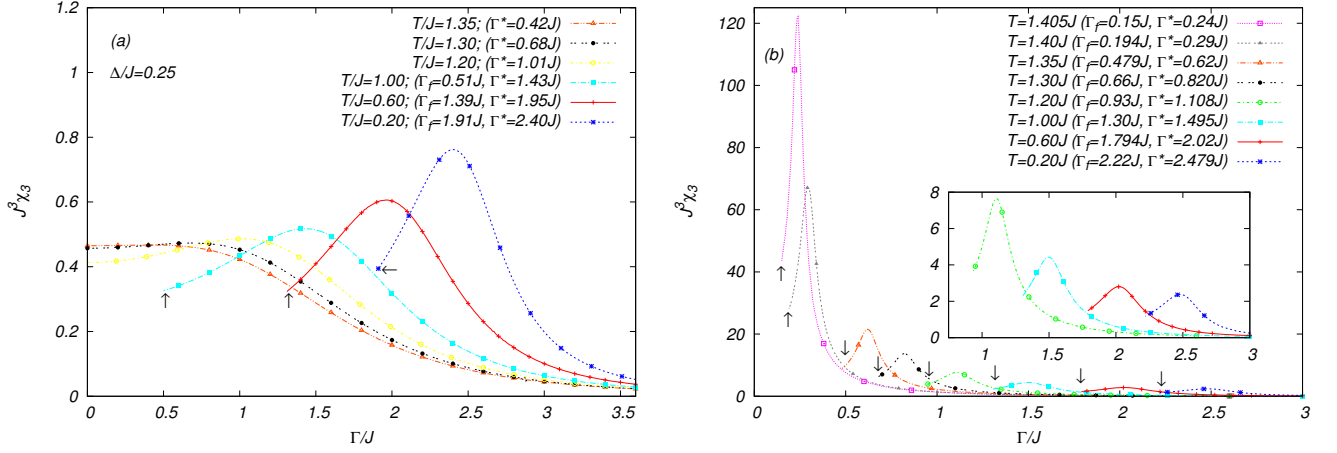


FIG. 4: (a) The dimensionless nonlinear susceptibility is represented versus  $\Gamma/J$ , for typical fixed temperatures and a nonzero width for the random fields [ $(\Delta/J) = 0.25$ ]. The divergences that occur for  $\Delta = 0$  at  $\Gamma_f(T)$  [following Eq. (6)], signalled by arrows in some cases, get smoothened due to the random fields, so that their corresponding maxima [located at  $\Gamma^*(T)$ ] are shifted towards higher values of the transverse field, i.e.,  $\Gamma^*(T) > \Gamma_f(T)$ . (b) The behavior of the dimensionless nonlinear susceptibility is shown versus  $\Gamma/J$ , for typical fixed temperatures, by considering a particular relation involving  $\Delta$  and  $\Gamma$  [ $(\Delta/J) = 0.02(\Gamma/J)^2$ ]; the inset represents an amplification of the region for higher values of  $\Gamma/J$ . In all cases, the maxima [located at  $\Gamma^*(T)$ ] appear shifted with respect to the onset of RSB [located at  $\Gamma_f(T)$ , signalled by arrows in some cases] towards higher values of the transverse field, i.e.,  $\Gamma^*(T) > \Gamma_f(T)$ .

like in Fig. 2(a), these divergences coincide with the onset of RSB indicated by the parameter  $\delta$ . One notices that, as one approaches zero temperature [cf., e.g., the case  $(T/J) = 0.2$ ], the divergence at  $\Gamma_f(T)$  approaches the one that occurs at the QCP,  $\Gamma_c^0 = 2\sqrt{2}J^{30}$ . In the inset of Fig. 2(b), the critical behavior described by Eq. (6) (represented by the dashed-dotted line) was fulfilled in both cases, showing a good agreement in the region  $0.001 < (\Gamma - \Gamma_f(T))/\Gamma_f(T) < 0.1$ , with the same exponent  $\delta' = 1$  for the two values of temperatures investigated,  $(T/J) = 0.2$  (full line) and  $(T/J) = 1.0$  (dashed line). Hence, similarly to the results of Fig. 2(a) concerning the critical exponent  $\gamma$  of Eq. (7), the present estimates of  $\delta'$  suggest that the temperature should not change the universality class of this later exponent.

In agreement with the previous study of the SK model in the presence of a Gaussian random field<sup>35</sup>, the smoothening of  $\chi_3$  is verified in Fig. 3 for the cases  $(\Delta/J) > 0$ . For instance, Fig. 3(a) displays  $\chi_3$  versus  $T/J$ , for increasing values of  $\Delta/J$ , in the case  $\Gamma = 0$ , showing that the divergent peak of the nonlinear susceptibility is replaced by a broad maximum at a temperature  $T^*$ . One observes that such a peak becomes smoother, decreasing its height for increasing values of  $\Delta/J$ . Particularly, in the inset of Fig. 3(a) one sees that the temperature range  $0.001 < (T - T^*)/T^* < 0.1$  no longer can be fitted by Eq. (7) with the critical exponent  $\gamma = 1.0$ , in the cases  $(\Delta/J) > 0$ . In a similar way, Fig. 3(b) shows  $\chi_3$  versus  $\Gamma/J$ , for  $(T/J) = 1.0$ , considering the same values for  $\Delta/J$  of Fig. 3(a); again, the peak of nonlinear susceptibility gets flattened due to the presence of an applied random field, now displaying a maximum at  $\Gamma^*$ . Consequently, in such cases the region

$0.001 < (\Gamma - \Gamma^*)/\Gamma^* < 0.1$  cannot be fitted by Eq. (6) with a critical exponent  $\delta' = 1.0$ , as shown in the inset of Fig. 3(b).

In Fig. 4 we represent the dimensionless nonlinear susceptibility  $\chi_3$  versus  $\Gamma/J$ , for typical fixed temperatures, in two cases: (a)  $\Gamma/J$  and  $\Delta/J$  as independent quantities [Fig. 4(a)]; (b) Imposing a relation involving  $\Delta$  and  $\Gamma$  [Fig. 4(b)]. In Fig. 4(a) we consider a fixed value for the width of the Gaussian random fields [ $(\Delta/J) = 0.25$ ], showing that the sharp SG transitions occurring for  $\Delta = 0$ , signaled by divergences of  $\chi_3$  at the corresponding critical values  $\Gamma_f(T)$  [according to Eq. (6) and shown by arrows in some curves], change into smooth curves with maxima at  $\Gamma^*(T)$ , shifted to higher values of  $\Gamma$ , i.e.,  $\Gamma^*(T) > \Gamma_f(T)$ . Following the proposal of Ref.<sup>22</sup>, for dealing properly with the experimental behavior of  $\chi_3$  in the  $\text{LiHo}_x\text{Y}_{1-x}\text{F}_4$  compound, we analyzed the present system by imposing a relation involving  $\Delta$  and  $\Gamma$ , i.e.,  $\Delta \equiv \Delta(\Gamma)$ . According to the experimental investigations of Ref.<sup>14</sup>, such a relation should satisfy certain requirements, e.g.,  $\Delta$  should increase monotonically with  $\Gamma$ , and one should get  $\Delta = 0$  for  $\Gamma = 0$ . The simplest proposal obeying these conditions comes to be a power function,  $(\Delta/J) = A(\Gamma/J)^B$ , where  $A$  and  $B$  are fitting parameters. Herein, these parameters were computed by adjusting our results to those of the experiments of Ref.<sup>14</sup>, leading to the optimal values  $A = 0.02$  and  $B = 2$ . In Fig. 4(b) we exhibit the dimensionless nonlinear susceptibility, versus  $\Gamma/J$ , for typical fixed temperatures, by considering this particular relation involving  $\Delta$  and  $\Gamma$ . In all cases, the maxima [located at  $\Gamma^*(T)$ ] appear shifted with respect to the onset of RSB [located at  $\Gamma_f(T)$ ] towards higher values of the transverse field, i.e.,  $\Gamma^*(T) > \Gamma_f(T)$ .

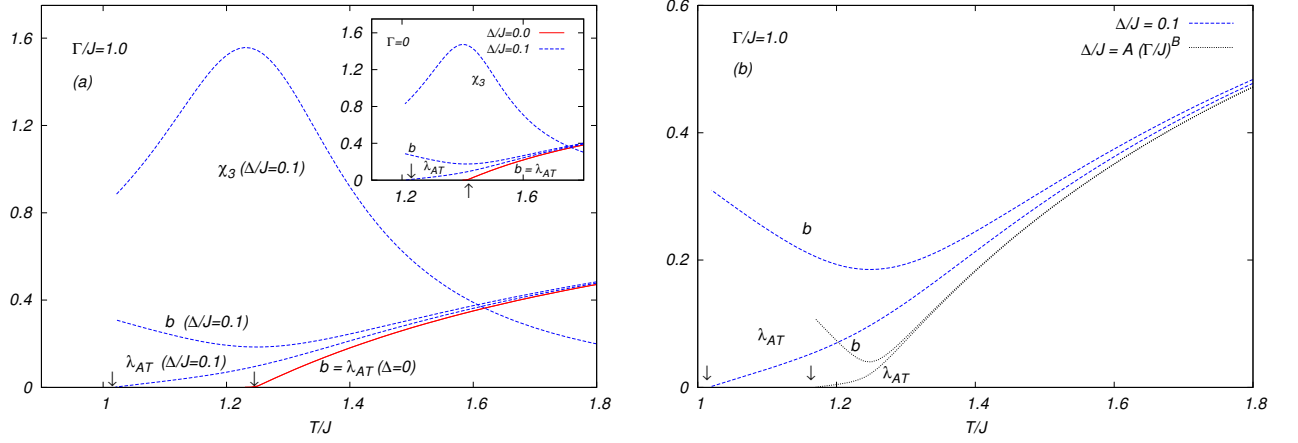


FIG. 5: The softening of the nonlinear susceptibility is illustrated by means of the denominator of  $q_2$ , i.e.,  $q_2 \propto b^{-1}$ ,  $b = 1 - 2(\beta J)^2 I_0(\Gamma)$  [cf. Eq. (24)], which appears in the expression of  $\chi_3$  calculated in Appendix A, within the RS approximation. The Almeida-Thouless eigenvalue  $\lambda_{AT}$ , associated with the onset of RSB and defining the SG critical temperature  $T_f$  is also shown, for comparison. (a) Results for  $(\Gamma/J) = 1.0$  are exhibited for two typical values of  $\Delta/J$ , namely,  $(\Delta/J) = 0.0$  and  $(\Delta/J) = 0.1$ , in the case where  $\Gamma$  and  $\Delta$  are independent; similar results are presented in the inset for  $(\Gamma/J) = 0$ . The full lines represent the cases  $(\Delta/J) = 0.0$ , showing that  $\lambda_{AT}$  and the denominator  $b$  coincide, becoming zero at the temperature  $T_f$ . The cases  $(\Delta/J) = 0.1$  show that  $b$  is always positive, presenting a smooth minimum around a temperature  $T^*$ , leading to the rounding of  $\chi_3$ , whereas  $\lambda_{AT}$  becomes zero at a lower temperature  $T_f$ . (b) Results for  $(\Gamma/J) = 1.0$  and  $(\Delta/J) = 0.1$  are shown, by comparing the case where these two quantities are considered as independent (dashed lines), with the one where they follow the relation proposed in in Fig. 4(b)  $[(\Delta/J) = 0.02(\Gamma/J)^2]$  (dotted lines). In all cases, the arrows locate the freezing temperature  $T_f$ .

The most important novelty of Fig. 4(b) [to be contrasted with the results of Fig. 4(a)], concerns the fact that the amplitude of the maximum of  $\chi_3$  decreases for increasing values of  $\Gamma/J$ , and consequently, for decreasing temperatures.

Recent studies in the compound  $\text{LiHo}_x\text{Y}_{1-x}\text{F}_4$  suggested that the transverse field  $\Gamma$  introduced in the Hamiltonian of Eq. (8) should be related to the experimental applied field in a real system,  $H_t^{11,12}$ ; in fact, at least for low  $H_t$ ,  $\Gamma \propto H_t^2$  (see, e.g., Ref.<sup>42</sup>). Hence, considering a new dimensionless variable,  $H_t$  ( $H_t \equiv \sqrt{\Gamma/J}$ ), we have verified that the same qualitative behavior shown in both Figs. 4(a) and 4(b) occur in representations of the dimensionless nonlinear susceptibility  $\chi_3$  versus  $H_t$ . Consequently, Fig. 4(b) preserves the agreement with experimental observations, showing that besides the progressive smearing of  $\chi_3$ , the amplitude of its maximum also decreases as the real field  $H_t$  increases, as suggested by Tabei and collaborators<sup>22</sup>.

In Appendix A we have calculated  $\chi_3$  analytically, within the RS approximation, for both  $\Gamma > 0$  [cf. Eqs. (A1) and (A2)] and  $\Gamma = 0$  [cf. Eq. (A13)]. In these calculations, an important quantity emerged, given in Eq. (A2) for  $\Gamma > 0$ , as

$$q_2 = \frac{2(\beta J)^2 I_0(\Gamma)}{b}; \quad b = 1 - 2(\beta J)^2 I_0(\Gamma). \quad (24)$$

Notice that the denominator  $b$  may become zero, leading to a divergence in the nonlinear susceptibility; it should be mentioned that  $q_2$  is the only quantity appearing in  $\chi_3$

[either in Eq. (A1), or in Eq. (A13)], which may present a divergence at finite temperatures. Moreover, one can show that for  $\Delta = 0$ , the so-called “dangerous” eigenvalue<sup>31</sup> in Eq. (A10) is equal to the denominator of  $q_2$ , i.e.,  $\lambda_{AT} = 1 - 2(\beta J)^2 I_0(\Gamma)$ , even for  $\Gamma > 0$ . The mechanism behind the flattening of the  $\chi_3$  peak at  $T^*$  is illustrated in Fig. 5, where we plot the quantity  $b$  of Eq. (24),  $\lambda_{AT}$ , and  $\chi_3$ , versus the dimensionless temperature, for typical choices of  $\Gamma/J$  and  $\Delta/J$ . Results for  $\Gamma$  and  $\Delta$  independent are presented in Fig. 5(a); the full lines [cases  $(\Delta/J) = 0.0$ ] show that the quantities  $b$  and  $\lambda_{AT}$  become zero together, being associated with the divergence of  $\chi_3$  [according to Eq. (7)], signalling the SG phase-transition temperature  $T_f$ . However, the results for  $(\Delta/J) = 0.1$  show that such a small value for the width of the RFs distribution yields  $b > 0$ , which presents a smooth minimum around a temperature  $T^*$ , being directly associated with the rounding behavior of  $\chi_3$ ; on the other hand, one has  $\lambda_{AT} = 0$  at a temperature  $T_f$ , with  $T_f < T^*$ . In Fig. 5(b) we present the denominator  $b$  and  $\lambda_{AT}$ , for the cases where  $\Gamma$  and  $\Delta$  are independent (dashed lines), and where these quantities are related through the power law  $(\Delta/J) = 0.02(\Gamma/J)^2$ . In this later case, since one has  $(\Delta/J) > 0$  for any  $(\Gamma/J) > 0$ , the denominator  $b$  will always display a minimum value around a temperature  $T^*$ , higher than  $T_f$ . Particularly, by means of this relation, higher values of  $\Gamma$  imply on higher values of  $\Delta$ , increasing the values of  $b$  at the minima, resulting in a decrease in the amplitude of the maxima of  $\chi_3$ .

In Fig. 6 we present phase diagrams  $T/J$  versus  $\Gamma/J$



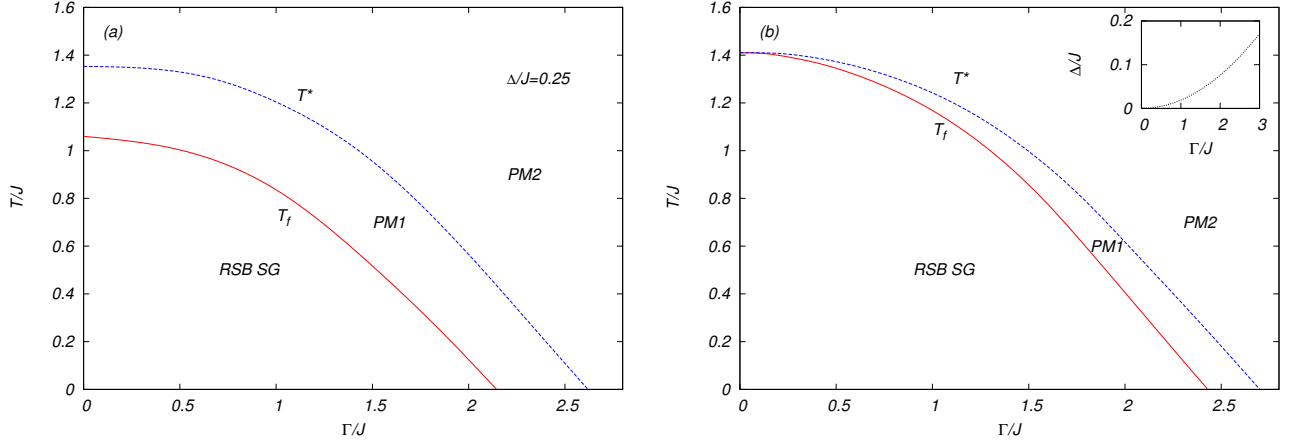


FIG. 6: Phase diagrams  $T/J$  versus  $\Gamma/J$  showing the frontiers separating the SG and paramagnetic phases (full lines), which represent the behavior of the temperature  $T_f$  for increasing values of  $\Gamma$ , located by the onset of RSB, i.e.,  $\lambda_{AT} = 0$ . The dashed lines correspond to the temperature  $T^*$ , associated with the maximum of the nonlinear susceptibility  $\chi_3$ , and herein interpreted as a crossover between two distinct regions of the paramagnetic phase (PM1 and PM2). (a) Phase diagram for  $(\Delta/J) = 0.25$ , in the case where  $\Gamma$  and  $\Delta$  are independent. (b) Phase diagram for which  $\Gamma$  and  $\Delta$  follow the relation proposed in Fig. 4(b)  $[(\Delta/J) = 0.02(\Gamma/J)^2]$ , whose parabolic behavior is presented in the inset. Due to the usual numerical difficulties, the low-temperature results [typically  $(T/J) < 0.05$ ] correspond to smooth extrapolations from higher-temperature data.

showing a decrease in the temperature  $T_f$  for increasing values of  $\Gamma$  (full lines). These lines delimit the SG phase and were identified with the onset of RSB, by setting  $\lambda_{AT} = 0$ ; throughout the whole SG phases one has  $\lambda_{AT} < 0$ . The temperature  $T^*$  (dashed lines), associated with the maximum of the nonlinear susceptibility  $\chi_3$ , signals a crossover between two regions of the paramagnetic phase (PM1 and PM2), as will be discussed next. The phase diagram shown in Fig. 6(a) corresponds to a fixed value of  $\Delta$   $[(\Delta/J) = 0.25]$ , and was obtained by considering  $\Gamma$  and  $\Delta$  as independent quantities. In this case, one notices that the two lines (full and dashed lines) remain essentially parallel to one another, up to zero temperature, where the full line reaches a QCP, which appears to be shifted towards lower values of  $\Gamma$ , when compared with the QCP for  $\Delta = 0$ ,  $\Gamma_c^0 = 2\sqrt{2}J \approx 2.828J$ <sup>40</sup>. The case shown in Fig. 6(b) corresponds to  $\Gamma$  and  $\Delta$  following the relation  $(\Delta/J) = 0.02(\Gamma/J)^2$  (see inset), so that for  $\Gamma = 0$ , one has  $\Delta = 0$ , giving  $T^* = T_f$ . By increasing values of  $\Gamma$ , the width of RFs also increases, leading to a rounded peak in the nonlinear susceptibility, yielding  $T^* > T_f$ , and consequently, the region PM1 emerges. Due to the joint increase of both  $\Gamma$  and  $\Delta$ , as shown in the inset, the region PM1 gets enlarged up to zero temperature, where one gets a QCP, shifted towards lower values of  $\Gamma$  as compared with the QCP for  $\Delta = 0$ , similarly to the one occurring in Fig. 6(a).

It should be emphasized that the temperature  $T^*$  plays a role different from  $T_f$ , in the sense that it does not correspond to a phase transition, but rather to a crossover between two distinct regions of the paramagnetic phase. The previous analysis of the SK model in the presence of a Gaussian random field Ref.<sup>35</sup>, which should correspond herein to the region of high temperatures and low

$\Gamma$  (i.e., the classical regime), has also found a temperature  $T^*$ , associated with the rounded maximum of  $\chi_3$ , with  $T^* > T_f$ . In this case,  $T^*$  was interpreted as an effect of the RFs acting inside the paramagnetic phase, instead of some type of non-trivial ergodicity breaking. Herein, we claim that the temperature  $T^*$ , although it may be also affected by the transverse field  $\Gamma$ , should be interpreted in a similar manner. Hence, along the line signaled by  $T_f$ , the growth of  $\Gamma$  produces an enhancement of quantum fluctuations, which become increasingly dominant as compared with thermal fluctuations, driving the non-trivial ergodicity breaking of the SG phase transition to a QCP. For temperatures in the region  $T_f < T < T^*$ , the enhancement of quantum fluctuations by  $\Gamma$  along with the spin fluctuations due to the RFs inside the paramagnetic phase create two distinct scenarios, more precisely concerning the PM1 region, as discussed next: (a) For fixed  $\Delta$  [e.g., Fig. 6(a)], one has  $\Gamma$  and  $\Delta$  independent, so that the smearing of the nonlinear susceptibility is caused only by the RFs, leading to the effect that the full and dashed lines remain essentially parallel to one another, up to zero temperature; (b) The phase diagram of Fig. 6(b), for which  $\Delta$  and  $\Gamma$  are related through the parabolic behavior shown in the inset, the appearance of  $T^*$  occurs for  $\Gamma > 0$  (i.e.,  $\Delta > 0$ ). Hence, the region PM1 starts very narrow for low  $\Gamma$ , and gets enlarged for increasing values of  $\Gamma$ , showing that the rounding of  $\chi_3$  is dominated by the enhancement of the RFs, leading to spins fluctuations due to the RFs inside the paramagnetic phase.

#### IV. CONCLUSIONS

We have investigated a quantum spin-glass model in the presence of a uniform transverse field  $\Gamma$ , as well as of a longitudinal random field  $h_i$ , the later following a Gaussian distribution characterized by a width proportional to  $\Delta$ . The model was considered in the limit of infinite-range interactions and studied through the replica formalism, within a one-step replica-symmetry-breaking procedure. The spin-glass critical frontier, signaled by the temperature  $T_f$ , was identified with the onset of replica-symmetry breaking, calculated through the Almeida-Thouless eigenvalue (replicon)  $\lambda_{AT}$ , i.e., by setting  $\lambda_{AT} = 0$ . In this approach, the whole spin-glass phase becomes characterized by  $\lambda_{AT} < 0$ , and consequently, it was treated through replica-symmetry breaking. Such analysis was motivated by experimental investigations on the  $\text{LiHo}_x\text{Y}_{1-x}\text{F}_4$  compound. In this system, the application of a transverse magnetic field yields rather intriguing effects, particularly related to the behavior of the nonlinear magnetic susceptibility  $\chi_3$ , which have led to a considerable experimental and theoretical debate.

We have analyzed two physically distinct situations, namely,  $\Delta$  and  $\Gamma$  considered as independent, as well as these two quantities related, as proposed recently by some authors (see, e.g., Ref.<sup>22</sup>). In both cases, we have found a spin-glass critical frontier, given by  $T_f \equiv T_f(\Gamma, \Delta)$ , with such phase being characterized by a nontrivial ergodicity breaking. In the first case, for  $\Delta$  fixed, we have found that  $T_f(\Gamma, \Delta)$  decreases by increasing  $\Gamma$  towards a quantum critical point at zero temperature, whereas in the second, we have found a similar behavior for this critical frontier, with  $\Delta$  changing according to variations in  $\Gamma$ . In this later case, we have taken into account previous experimental investigations<sup>14</sup> which suggest that a relation of the type  $\Delta \equiv \Delta(\Gamma)$  should satisfy certain requirements, e.g.,  $\Delta$  should increase monotonically with  $\Gamma$ , and one should get  $\Delta = 0$  for  $\Gamma = 0$ . Although such a relation may not be unique, the simplest proposal following such conditions appears to be a power function,  $(\Delta/J) = A(\Gamma/J)^B$ . In the present work, the parameters  $A$  and  $B$  were computed by adjusting our results to those of the experiments of Ref.<sup>14</sup>, leading to the optimal values  $A = 0.02$  and  $B = 2$ .

We have shown that the present approach, considering the relation  $(\Delta/J) = 0.02(\Gamma/J)^2$ , was able to reproduce adequately the experimental observations on the  $\text{LiHo}_x\text{Y}_{1-x}\text{F}_4$  compound, with theoretical results coinciding qualitatively with measurements of the nonlinear susceptibility  $\chi_3$ . As a consequence, by increasing  $\Gamma$  gradually, our results indicate that  $\chi_3$  becomes progressively rounded, presenting a maximum at a temperature  $T^*$  ( $T^* > T_f$ ); moreover, both amplitude of the maximum and the value of  $T^*$  diminish, by enhancing  $\Gamma$ .

From the analysis where  $\Delta$  and  $\Gamma$  are considered as independent, we have concluded that the random field is the main responsible for the smearing of the nonlinear

susceptibility. Hence, the random field acts significantly inside the paramagnetic phase, leading to two regimes delimited by the temperature  $T^*$ , one for  $T_f < T < T^*$  (called herein as PM1), and another one for  $T > T^*$  (denominated as PM2). In the paramagnetic regime for  $T > T^*$  one should have weak correlations and consequently, the usual paramagnetic type of behavior. However, close to  $T^*$ , and particularly for temperatures in the range  $T_f < T < T^*$ , one expects a rather nontrivial behavior in real systems, as happens with experiments in the compound  $\text{LiHo}_x\text{Y}_{1-x}\text{F}_4$ , resulting in very controversial interpretations<sup>11,16,17,20–24</sup>. Hence, as already argued in the analysis of the SK model in the presence of Gaussian random field<sup>35</sup>, the line PM1–PM2 may not characterize a real phase transition, in the sense of a diverging  $\chi_3$ , but the region PM1 should be certainly characterized by a rather nontrivial dynamics. As one possibility, one should have a growth of free-energy barriers in this region, leading to a slow dynamics, whereas only below  $T_f$  the nontrivial ergodicity breaking appears, typical of RSB in SG systems. Also, one could have Griffiths singularities along PM1, which are found currently in disordered magnetic systems, like site-diluted ferromagnets<sup>43</sup>, ferromagnet in a random field<sup>44</sup>, classical Ising spin glasses<sup>45</sup>, and also claimed to occur in quantum spin glasses<sup>46–48</sup>. Whether such curious properties may appear throughout the region PM1 in the present problem, represents a matter for further investigation. In fact, recent experiments in the above compound for  $x = 0.045$  strongly suggest this picture<sup>49</sup>: these authors claim an “unreachable” transition due to an ultra-slow dynamics (of the order  $10^7$  times slower than the ones of conventional spin-glass materials) and argue that such a dynamics should be caused by a Griffiths phase between the paramagnetic and spin-glass phases.

Next, we discuss some contributions of the present work, as compared to previous theoretical approaches in this problem. (i) The analysis of Ref.<sup>27</sup> did not take into account the random field, which in our view, represents a key ingredient for an appropriate description of the properties of  $\text{LiHo}_x\text{Y}_{1-x}\text{F}_4$ . Moreover, as it was shown herein, the RSB SG parameters, together with the magnetization  $m$ , and the quadrupolar parameter  $p$ , all form a set of coupled equations, to be solved simultaneously. The approach of Ref.<sup>27</sup> considered  $p$  as independent from the remaining parameters; this could be directly related with the curious result concerning a part of the SG phase characterized by stability of the replica-symmetric solution, along which these authors find the rounded maximum of  $\chi_3$ . (ii) The study of Ref.<sup>22</sup> has considered an effective Hamiltonian characterized by an extra two-body interacting term (as compared with the Hamiltonian used herein), coupling spin operators in the  $x$  and  $z$  directions. Moreover, these authors have suggested a relation  $\Delta \equiv \Delta(\Gamma)$ , which due to the Hamiltonian employed, turned out to be slightly different from ours, e.g.,  $(\Delta/J) = A(\Gamma/J)^B$ , with an exponent  $B < 1$ . The results obtained herein for the nonlinear susceptibil-

ity  $\chi_3$  corroborate those of Ref.<sup>22</sup>; however, we understand that the present analysis, characterized by a single two-body interacting term,  $-\sum_{(i,j)} J_{ij} \hat{S}_i^z \hat{S}_j^z$ , leads to a much simpler analysis to the problem, when compared to the one carried in this previous work.

To conclude, we have considered a model able to reproduce theoretically many properties observed in experiments on the  $\text{LiHo}_x\text{Y}_{1-x}\text{F}_4$  compound, particularly those related to the nonlinear susceptibility  $\chi_3$ . The present theoretical proposal appears to be simpler than previous ones, and consequently, its results should be easier to compare with further experimental investigations. Obviously, the observation of a clear spin-glass state, characterized by a nontrivial ergodicity breaking at a temperature  $T_f$  (below the temperature  $T^*$  where one observes rounded effects on the nonlinear susceptibility) represents a challenge for experiments.

### Acknowledgments

We acknowledge the partial financial support from CNPq, FAPERGS, FAPERJ, and CAPES (Brazilian funding agencies).

### Appendix A: Nonlinear Susceptibility in the RS Solution

In this appendix we obtain the nonlinear susceptibility  $\chi_3$  analytically for the 2S model, within the RS solution. Although in the RS solution, these results allow us to analyze in detail how the RFs and the transverse field  $\Gamma$  affect the nonlinear susceptibility. Particularly, one has that the nonlinear susceptibility of Eq. (3) becomes

$$\begin{aligned} \chi_3 &= -\frac{1}{3!} \left. \frac{\partial^3 m}{\partial H_l^3} \right|_{H_l \rightarrow 0} \\ &= \frac{\beta^3}{3} [1 + 3q_2 + 2(\beta J)^2 V_3] \frac{-V_2}{2 - 2(\beta J)^2 V_3}, \end{aligned} \quad (\text{A1})$$

where

$$q_2 = \frac{2(\beta J)^2 I_0(\Gamma)}{1 - 2(\beta J)^2 I_0(\Gamma)}, \quad (\text{A2})$$

with the following definitions

$$I_0(\Gamma) = \frac{V_3 - V_2}{2} + 2(\beta J)^2 \frac{V_2 V_1}{2 - 2(\beta J)^2 V_3}, \quad (\text{A3})$$

$$V_1 = \int Dz \left[ \frac{C_3 C_1}{K^2} - \frac{C_2 (C_1)^2}{K^3} \right], \quad (\text{A4})$$

$$\begin{aligned} V_2 &= \int Dz \left[ \frac{C_4}{K} - 4 \frac{C_3 C_1}{K^2} - 3 \left( \frac{C_2}{K} \right)^2 \right. \\ &\quad \left. + 12 \frac{C_2 (C_1)^2}{K^3} - 6 \left( \frac{C_1}{K} \right)^4 \right], \end{aligned} \quad (\text{A5})$$

$$V_3 = \int Dz \left[ \frac{C_4}{K} - 2 \frac{C_3 C_1}{K^2} - \left( \frac{C_2}{K} \right)^2 + 2 \frac{C_2 (C_1)^2}{K^3} \right]. \quad (\text{A6})$$

In the equations above, one has that

$$C_n = \int D\xi \frac{\partial^n f(h)}{\partial h^n}; \quad K = \int D\xi f[h(z, \xi), \Gamma], \quad (\text{A7})$$

with

$$f[h(z, \xi), \Gamma] = \cosh \sqrt{h^2(z, \xi) + (\beta \Gamma)^2}, \quad (\text{A8})$$

and

$$h(z, \xi) = \beta J [\sqrt{2q + (\Delta/J)^2} z + \sqrt{2(p-q)} \xi]. \quad (\text{A9})$$

In addition, the limit of stability of the RS solution is delimited by  $\lambda_{\text{AT}} > 0$ <sup>31</sup>, which may be expressed in terms of the above quantities as

$$\lambda_{\text{AT}} = 1 - 2(\beta J)^2 \int Dz \left[ \frac{C_2}{K} - \left( \frac{C_1}{K} \right)^2 \right]^2. \quad (\text{A10})$$

The particular case  $\Gamma = 0$  gives

$$h_0(z) = \beta J (\sqrt{2q + (\Delta/J)^2} z), \quad (\text{A11})$$

as well as  $V_1 = V_3 = 0$ , whereas

$$V_2 = -2 \int Dz [\text{sech}^4 h_0(z) - 2 \tanh^2 h_0(z) \text{sech}^2 h_0(z)]. \quad (\text{A12})$$

As a result,  $\chi_3$  becomes

$$\chi_3 = \frac{\beta^3}{3} [1 + 3q_2] I_0(0) \quad (\text{A13})$$

where  $q_2 = [2(\beta J)^2 I_0(0)]/[1 - 2(\beta J)^2 I_0(0)]$  and

$$I_0(0) = \int Dz [\text{sech}^4 h_0(z) - 2 \tanh^2 h_0(z) \text{sech}^2 h_0(z)]. \quad (\text{A14})$$

In this case,  $\chi_3$  coincides with the one found in Ref.<sup>35</sup>.

\* Electronic address: sgmagal@gmail.com

<sup>1</sup> W. Nolting and A. Ramakanth, *Quantum Theory of Mag-*

- netism* (Springer-Verlag, Berlin, 2009).
- <sup>2</sup> K. Binder and A. P. Young, *Rev. Mod. Phys.* **58**, 801 (1986).
  - <sup>3</sup> K. H. Fischer and J. A. Hertz, *Spin Glasses* (Cambridge University Press, Cambridge, UK, 1991).
  - <sup>4</sup> V. Dotsenko, *Introduction to the Replica Theory of Disordered Statistical Systems* (Cambridge University Press, Cambridge, UK, 2001).
  - <sup>5</sup> H. Nishimori, *Statistical Physics of Spin Glasses and Information Processing* (Oxford University Press, Oxford, UK, 2001).
  - <sup>6</sup> D. Sherrington and S. Kirkpatrick, *Phys. Rev. Lett.* **35**, 1792 (1975).
  - <sup>7</sup> G. Parisi, *J. Phys. A* **13**, 1101 (1980); *ibid.* 1887 (1980).
  - <sup>8</sup> S. Sachdev, *Quantum Phase Transitions*, second edition (Cambridge University Press, Cambridge, UK, 2011).
  - <sup>9</sup> D. Bitko, T. F. Rosenbaum, and G. Aeppli, *Phys. Rev. Lett.* **77**, 940 (1996); P. B. Chakraborty, P. Henelius, H. Kjønsberg, A. W. Sandvik, and S. M. Girvin, *Phys. Rev. B* **70**, 144411 (2004).
  - <sup>10</sup> W. Wu, B. Ellman, T. F. Rosenbaum, G. Aeppli, and D. H. Reich, *Phys. Rev. Lett.* **67** 2076 (1991).
  - <sup>11</sup> M. Gingras, P. Henelius, *J. Phys: Conf. Ser.* **320**, 012001 (2011).
  - <sup>12</sup> J. A. Quilliam, S. Meng, J. B. Kycia, *Phys. Rev. B* **85**, 184415 (2012)
  - <sup>13</sup> J. Chalupa, *Sol. Stat. Comm.* **22**, 315 (1977).
  - <sup>14</sup> W. Wu, D. Bitko, T. F. Rosenbaum, and G. Aeppli, *Phys. Rev. Lett.* **71** 1919 (1993).
  - <sup>15</sup> L. F. Cugliandolo, D. R. Grempel, C. A. da Silva Santos, *Phys. Rev. B* **64**, 014403 (2001).
  - <sup>16</sup> P. E. Jönsson, R. Mathieu, W. Wernsdorfer, A. M. Tkachuk, B. Barbara, *Phys. Rev. Lett.* **98**, 256403 (2007).
  - <sup>17</sup> C. Ancona-Torres, D. M. Silevitch, G. Aeppli, T. F. Rosenbaum, *Phys. Rev. Lett.* **101**, 057201 (2008).
  - <sup>18</sup> J. F. Fernandez, *Phys. Rev. B* **82**, 144436 (2010).
  - <sup>19</sup> J. J. J. Alonso, *Phys. Rev. B* **91**, 094406 (2015).
  - <sup>20</sup> M. Schechter and N. Laflorencie, *Phys. Rev. Lett.* **97**, 137204 (2006).
  - <sup>21</sup> M. Schechter and P. C. E. Stamp, *Phys. Rev. Lett.* **95**, 267208 (2005).
  - <sup>22</sup> S. M. A. Tabei, M. J. P. Gingras, Y.-J. Kao, P. Stasiak and J.-Y. Fortin, *Phys. Rev. Lett.* **97**, 237203 (2006).
  - <sup>23</sup> S. M. A. Tabei, F. Vernay, M. J. P. Gingras, *Phys. Rev. B* **77**, 014432 (2008).
  - <sup>24</sup> J. A. Mydosh, *Rep. Prog. Phys.* **78**, 052501 (2015).
  - <sup>25</sup> D. S. Fisher, D. A. Huse, *Phys. Rev. Lett.* **56**, 1601 (1986).
  - <sup>26</sup> A. P. Young, H. G. Katzgraber, *Phys. Rev. Lett.* **93**, 207203 (2004).
  - <sup>27</sup> D. -H. Kim, J. -J. Kim, *Phys. Rev. B* **66**, 054432 (2002).
  - <sup>28</sup> Y. Y. Goldschmidt, P.-Y. Lai, *Phys. Rev. Lett.* **64**, 2467 (1990).
  - <sup>29</sup> J. Miller, D. A. Huse, *Phys. Rev. Lett.* **70**, 3147 (1993).
  - <sup>30</sup> N. Read, S. Sachdev and J. Ye, *Phys. Rev. B* **52**, 384 (1995).
  - <sup>31</sup> J. R. L. de Almeida, D. J. Thouless, *J. Phys. A* **11**, 983 (1978).
  - <sup>32</sup> T. Schneider, E. Pytte, *Phys. Rev. B* **15**, 1519 (1977)
  - <sup>33</sup> F. Krzakala, F. Ricci-Tersenghi, L. Zdeborova, *Phys. Rev. Lett.* **104**, 207208 (2010).
  - <sup>34</sup> R. F. Soares, F. D. Nobre and J. R. L. de Almeida, *Phys. Rev. B* **50**, 6151 (1994).
  - <sup>35</sup> C. V. Morais, F. M. Zimmer, M. J. Lazo, S. G. Magalhães, F. D. Nobre, *Phys. Rev. B* **93**, 224206 (2016).
  - <sup>36</sup> A. Theumann, M. V. Gusmão, *Phys. Lett. A* **105**, 311 (1984).
  - <sup>37</sup> R. Oppermann, A. Muller-Groeling, *Nuclear Phys. B* **401**, 507 (1993).
  - <sup>38</sup> A.J. Bray, M.A. Moore, *J. of Phys. C: Sol. State* **13**, L655 (1980).
  - <sup>39</sup> W. Wiethege and D. Sherrington, *J. Phys. C* **19** 69832 (1986)
  - <sup>40</sup> F. M. Zimmer, S. G. Magalhaes, *Phys. Rev. B* **74**, 012202 (2006).
  - <sup>41</sup> D. Thihumalai, Q. Li, and T. R. Kirkpatrick, *J. Phys. A* **22**, 3339 (1989).
  - <sup>42</sup> W. Wu, B. Ellman, T. F. Rosenbaum, G. Aeppli, D. H. Reich, *Phys. Rev. Lett.* **67**, 2076 (1991).
  - <sup>43</sup> R.B. Griffiths, *Phys. Rev. Lett.* **23**, 17 (1969).
  - <sup>44</sup> V. Dotsenko, *J. Stat. Phys.* **122**, 197 (2006); V. Dotsenko, *J. Phys. A: Math Gen.* **27**, 3397 (1994).
  - <sup>45</sup> M. Randeria, J. P. Sethna, and R.G. Palmer, *Phys. Rev. Lett.* **54**, 1321 (1985).
  - <sup>46</sup> M. Guo, R. N. Bhatt, D. A. Huse, *Phys. Rev. B* **54**, 3336 (1996).
  - <sup>47</sup> H. Rieger, A. P. Young, *Phys. Rev. B* **54**, 3328 (1996).
  - <sup>48</sup> A. P. Young, H. Rieger, *Phys. Rev. B* **53**, 8486 (1996).
  - <sup>49</sup> A. Biltmo and P. Henelius, *Nature Comm.* **3**:857 (2012).